Electronic Supplementary Material (ESI) for CrystEngComm.

Supplementary Information

Green Synthesis of Zirconium-MOFs

Helge Reinsch,[a] Bart Bueken,[b] Frederik Vermoortele,[b] Ivo Stassen,[b] Alexandra Lieb,[c] Karl-Petter Lillerud [a] and Dirk De Vos[b]

[a] Department of Chemistry, University of Oslo, P.O. Box 1033 Blindern, 0315 Oslo, Norway.

[b] Centre for Surface Chemistry and Catalysis, University of Leuven, Kasteelkpark Arenberg 23, 3001 Heverlee, Belgium. Fax: +32 16 3 21998; Tel: +32 16 32 16 39; E-mail: dirk.devos@biw.kuleuven.be.

[c] Institut für Chemie, Otto-von-Guericke-Universität Magdeburg, Universitätsplatz 2, 39106, Magdeburg, Germany.

Experimental.

High-resolution PXRD data were collected from glass capillaries (diameter 0.7 mm) on a PANalytical Empyrean diffractometer (CuK_{α}-radiation) in transmission geometry. Thermogravimetric experiments were carried out under a flow of oxygen on a TA instruments Q500 with a heating rate of 10 K/min. IR-spectra were measured on a Bruker IFS 66 v/s using KBr discs. The IR-spectra of the adsorption of acetonitrile were measured on a Nicolet 6700 FTIR spectrometer. EDX-data were measured using a Philips ESEM XL30 after sputtering of the samples with carbon. Force-field calculations for structural optimisation were performed using Materials Studio[i] and all processing of PXRD data was carried out using TOPAS Academics.[ii] Nitrogen sorption isotherms were measured at 77 K. The specific surface area was evaluated by the BET-method and the micropore volume was calculated using the t-plot method.

Synthesis.

For the synthesis of (**1**) $[Zr_6(OH)_{10.8}(SO_4)_{3.6}(BDC\text{-}NH_2)_3(H_2O)_{7.4}]\cdot nH_2O$, 2400 mg (13.3 mmol) 2-aminoterephthalic acid ($H_2BDC\text{-}NH_2$), 7100 mg (20 mmol) $Zr(SO_4)_2\cdot 4H_2O$, 100 mL H_2O and 1 mL formic acid were heated at 98 °C under stirring for 16 h in a pyrex glass bottle placed in an oil bath. After cooling down to room temperature, the mixture was filtrated, washed with water and acetone and dried under ambient conditions. To restore the crystallinity after thermal activation, the product which had been dried at 150 °C in air was treated in 2 vol% sulfuric acid in water (5 mL liquid per 100 mg) at 60 °C overnight.

For the synthesis of (**2**) $[Zr_6(OH)_{14}(BDC\text{-}(CO_2H)_2)_4(H_2O)_2(SO_4)]\cdot nH_2O$, 6800 mg (26.8 mmol) pyromellitic acid ($H_2BDC\text{-}(COOH)_2$), 14200 (40 mmol) mg $Zr(SO_4)_2\cdot 4H_2O$, 80 mL H_2O and 2 mL sulfuric acid were heated at 90 °C under stirring for 16 h in a pyrex glass bottle placed in an oil bath. After cooling down to room temperature, the mixture was filtrated, washed with water and acetone and dried under ambient conditions. To restore the crystallinity after thermal activation, the product which had been dried at 150 °C in air was treated in 3 vol% sulfuric acid in water (5 mL liquid per 100 mg) at 60 °C overnight.

For the synthesis of (**3**) $[Zr_6O_2(OH)_6(BDC\text{-}F_4)_6(SO_4)]\cdot nH_2O\cdot 1.2H_2BDC\text{-}F_4$, 240 mg (1 mmol) tetrafluoroterephthalic acid ($H_2BDC\text{-}F_4$), 355 mg (1 mmol) $Zr(SO_4)_2\cdot 4H_2O$, 5 mL H_2O and 50 µL sulfuric acid were heated at 90 °C under stirring for 16 h in a crimp cap vial. After cooling down to room temperature, the mixture was filtrated, washed with water and acetone and dried under ambient conditions.

The composition of the products is proposed based on the PXRD-data, IR spectra, TG curves and EDX spectroscopy. All data were measured for the as-synthesised compounds without further activation. The ratios of Zr:S determined by EDX-spectroscopy were 6:3.6 for (**1**), 6:1 for (**2**) and 6:1 for (**3**). Treatment of the solids in water at 90 °C leads to a ratio of 6:3 for (**1**), a virtually unchanged ratio in (**3**) and the removal of sulfate in (**2**). However, the number of O^{2-} and OH^- ions and water molecules which are part of the inorganic cluster core can vary and the proposed formulas must be considered as tentative.

Structure determination and Rietveld refinements.

The powder pattern of **1** could be indexed with a tetragonal cell (a = b = 14.230(3) Å, c = 21.414(2) Å) consistent with the extinction conditions for space group *I*-4 (No. 82). This space group is related to the one of UiO-66 (*Fm*-3*m*) by supergroup-subgroup relationships and since the pattern showed strong similarities with the one of UiO-66, a starting model was developed starting from the crystal structure of UiO-66. In a first step the symmetry was changed in the sequence *Fm*-3*m* -> *I*4/*mmm* -> *I*-42*m* -> *I*-4 using the Powdercell software.[iii] This first model was further manipulated employing the Materials Studio software package. The indexed cell parameters were adapted and the linker molecules in the equatorial plane of the inorganic node were removed. Subsequently the functional groups and the sulphate ions were added to the model and the hypothetical structure was optimised by force-field calculations (Universal force-field). This second model was employed as starting point for Rietveld refinement. The linker molecules were refined as rigid bodies and their occupancy was refined in consistence with the TG data. All other atoms were freely refined. Residual electron density in the framework's cavities was attributed to partially occupied oxygen atoms representing water molecules. The final structure showed an ordering of the NH_2-group and two possible positions for the sulphate ions.

The powder pattern of **2** could also be indexed with a tetragonal cell (a = b = 14.172(2) Å, c = 21.297(2) Å) consistent with the extinction conditions for space group *I*-4. This indicated a structure isoreticular to **1** and therefore the refined crystal structure of **1** was used as initial starting model. The NH_2-groups were replaced by COO-groups and the indexed cell parameters were adapted. Subsequently the model was optimised by force-field methods and the resulting structure was employed as starting point for Rietveld refinement. The linker molecules were treated as rigid bodies and their occupancy was constrained to values consistent with the analytical data, while all other atoms were freely refined. Again an ordering of the functional groups could be observed. However, the data did not allow for the localisation of the sulphate ions. Residual electron density was attributed to partially occupied oxygen atoms representing water molecules.

The powder pattern of **3** unambiguously indicated a structure isoreticular to UiO-66. A starting model for Rietveld refinement was set up by adding the F-atoms to the crystal structure of UiO-66 and subsequent optimisation by force-field methods using Materials Studio. During the refinement the residual electron density within the pores was attributed to partially occupied oxygen atoms representing water molecules. However, the refinement only converged after allowing for a disorder of the linker molecules over two positions. Eventually all atoms were freely refined.

It should be mentioned that the attribution of residual electron density to oxygen atoms is not unambiguous and that the atoms generated in such a way should be rather considered as placeholders for any kind of guest molecules inside the pores. Especially in the case of **2** it is very difficult to discriminate between linker molecules that are part of the framework and linker molecules that are occluded inside the cavities, even when all analytical data are taken into account. Therefore the given compositions should be considered to be approximate values. The final Rietveld plots are shown in Figures S1-S3 and some relevant parameters are summarised in Table S1.

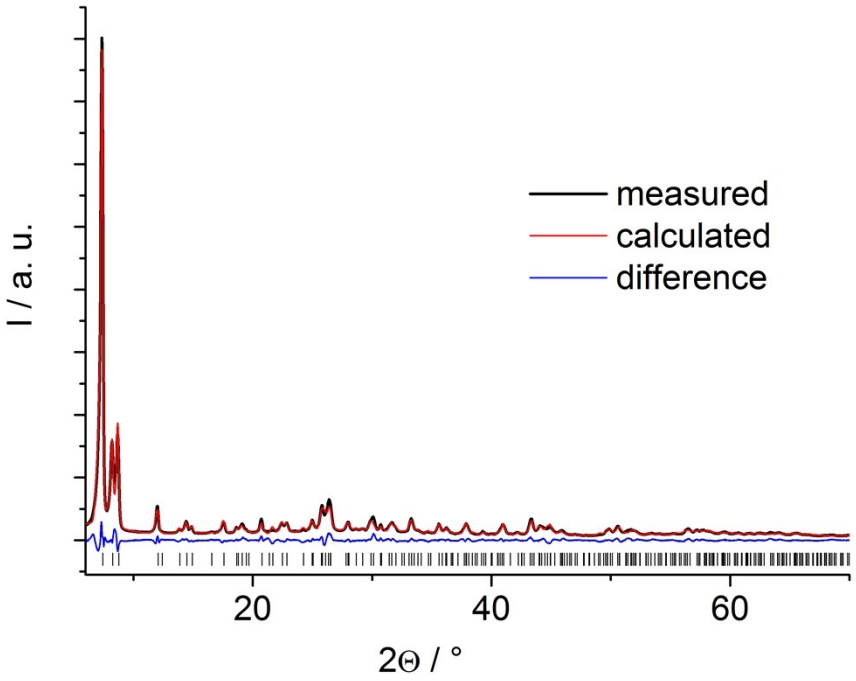

Figure S1: Rietveld plot for **1**. The black line is the experimental data, the red line the calculated data, the blue line gives the difference plot and the vertical bars mark the allowed peak positions.

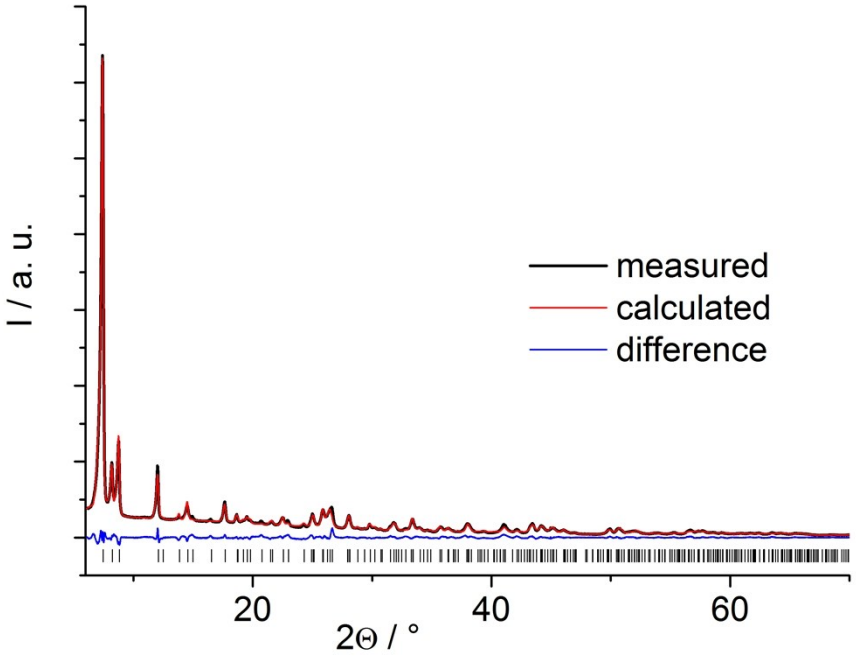

Figure S2: Rietveld plot for **2**. The black line is the experimental data, the red line the calculated data, the blue line gives the difference plot and the vertical bars mark the allowed peak positions.

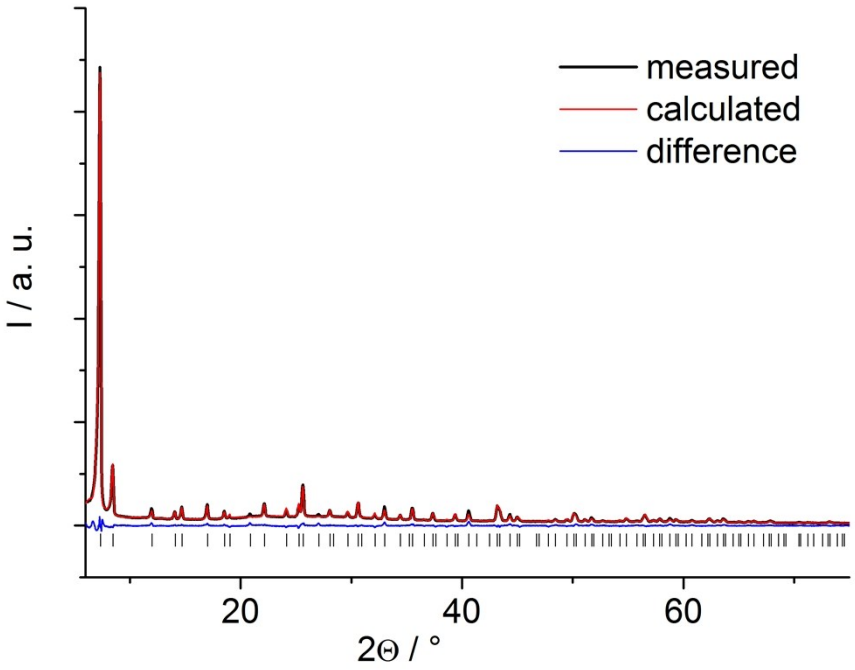

Figure S3: Rietveld plot for **3**. The black line is the experimental data, the red line the calculated data, the blue line gives the difference plot and the vertical bars mark the allowed peak positions.

Table S1: Some relevant parameters of the Rietveld-refinements for **1**-**3**.

compound	**1**	**2**	**3**
space group	*I*-4	*I*-4	*Fm*-3*m*
a / Å	14.248(1)	14.1669(8)	20.8253(4)
b / Å	14.248(1)	14.1669(8)	20.8253(4)
c / Å	21.369(3)	21.421(2)	20.8253(4)
$\alpha = \beta = \gamma$ / °	90	90	90
V / Å^3	4338.0(8)	4299.2(5)	9031.8(3)
R_{WP}/%	8.1	5.9	5.7
R_{Bragg}/%	4.2	1.8	2.6
GoF	5.3	5.6	3.6

Thermal behaviour.

The thermogravimetric curves are shown in Figure S4. In all three cases, water molecules are removed in a first step up to 200 °C. Beginning with the second step the frameworks decompose.

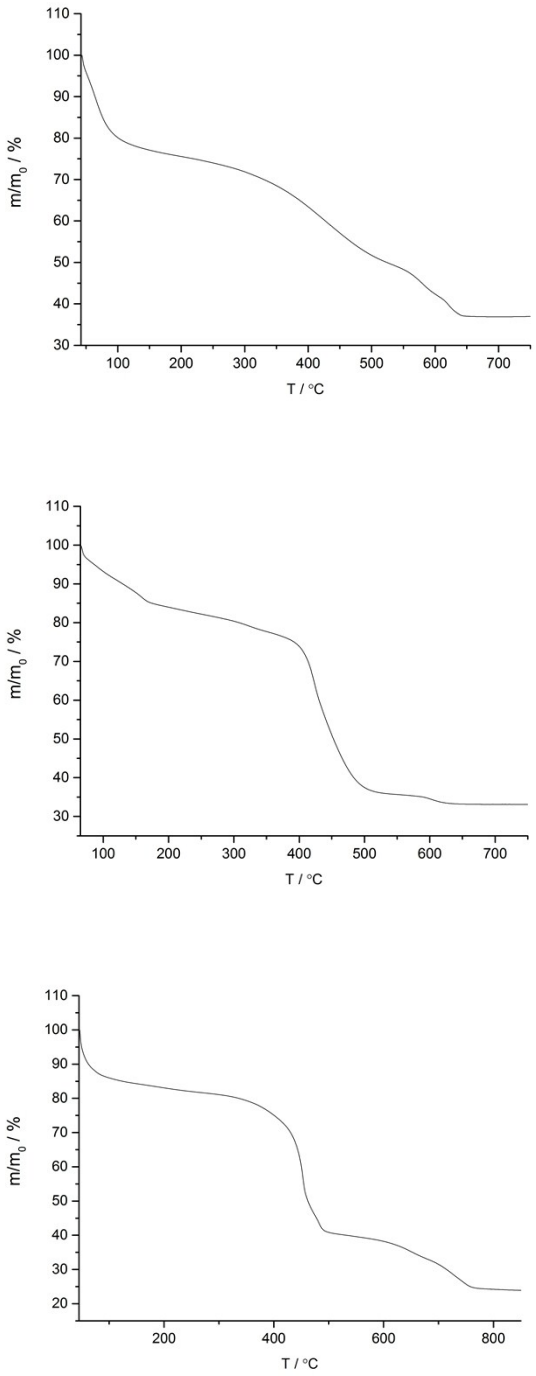

Figure S4: TG curves for (from top to bottom) **1**, **2** and **3** measured with a heating rate of 10 K/min under oxygen.

Table S2: Step sizes observed in the TG curves for compounds **1** - **3**.

compound	(**1**)	(**2**)	(**3**)
mass loss till 200 °C	24 %	16 %	17 %
corresponding to *n* H_2O	≈ 20	≈ 18	≈ 29
mass loss above 200 °C	40 %	51 %	59 %
expected mass loss above 200°C	44 %	53 %	60 %

The composition of the respective frameworks was deduced combining the Zr:S ratio and the mass loss observed in the second step of the TG curve. Moreover we assumed that all water molecules are removed from the framework at 200 °C, including the ones coordinated to the inorganic cluster. These data also indicated that substantial amounts of tetrafluoroterephthalic acid are occluded inside the cavities of **3**.

IR spectroscopy

The IR spectra of compounds **1**-**3** measured as KBr pellets under vacuum are shown in Figure S5.

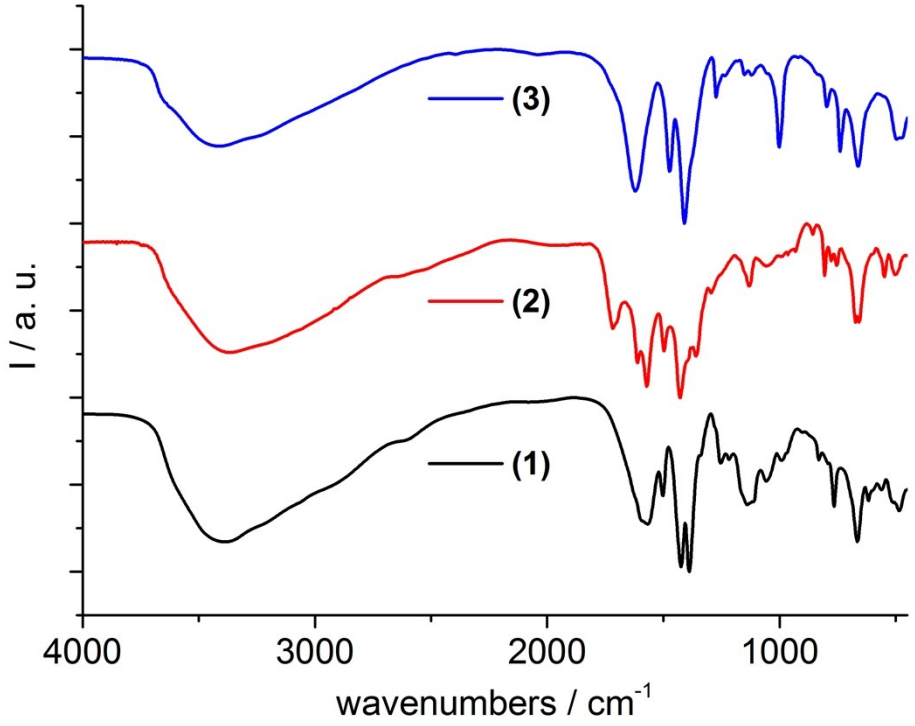

Figure S5: IR spectra for (from bottom to top) **1**, **2** and **3**.

For all three compounds the broad band around 3500 cm^{-1} attributed to ν-OH-vibrations indicates the presence of large amounts of water molecules occluded inside the framework. In the region around 1600 cm^{-1} only one broad band is visible for **1** at ≈ 1590 cm^{-1}. Thus the presence of protonated carboxylic acid groups due to inclusion of unreacted linker molecules can be excluded. In the spectrum of **2**, a signal at 1716 cm^{-1} proves the presence of such free carboxylic acid groups. In this case they are – at least mostly – part of the linker molecules as pyromellitic acid was used. However, the presence of unreacted linker molecules cannot be excluded from the data. The corresponding band for the asymmetric carbonyl-vibration in the spectrum of **3** is centered at 1624 cm^{-1}. A shoulder at 1720 cm^{-1} of asymmetric carbonyl vibrations of COOH-groups substantiates the assumption that protonated, unreacted linker molecules are still present in the framework as it was deduced from the TG data.

Upon thermal activation at 150 °C, a broadening of the signals is observed for **1** and **2**. In addition to this, a new band of very low intensity appears in the spectrum of **2** at ≈ 1850 cm^{-1} (Fig. S6). We attribute this band to carbonyl vibrations of anhydride groups.

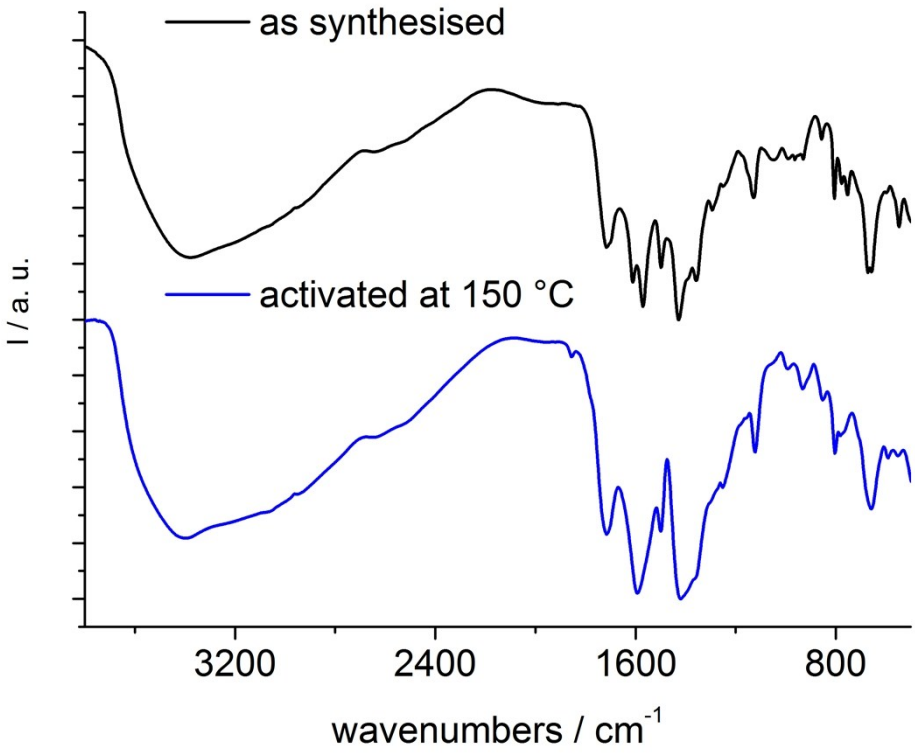

Figure S6: IR spectra for as synthesised (black line) and thermally activated (blue line) **2**.

Such groups can be formed in MOFs by the condensation of free carboxylic acid groups as it was already observed.[iv] This means that in **2** the reactivity of the functional groups might have an impact of the mechanism of amorphisation upon thermal treatment while in **1** the amorphisation should be mostly due to the highly heterogeneous structure.

In Figure S7 the region of interest for the adsorption of deuterated acetonitrile on **3** after activation at 220 °C in vacuum is shown.

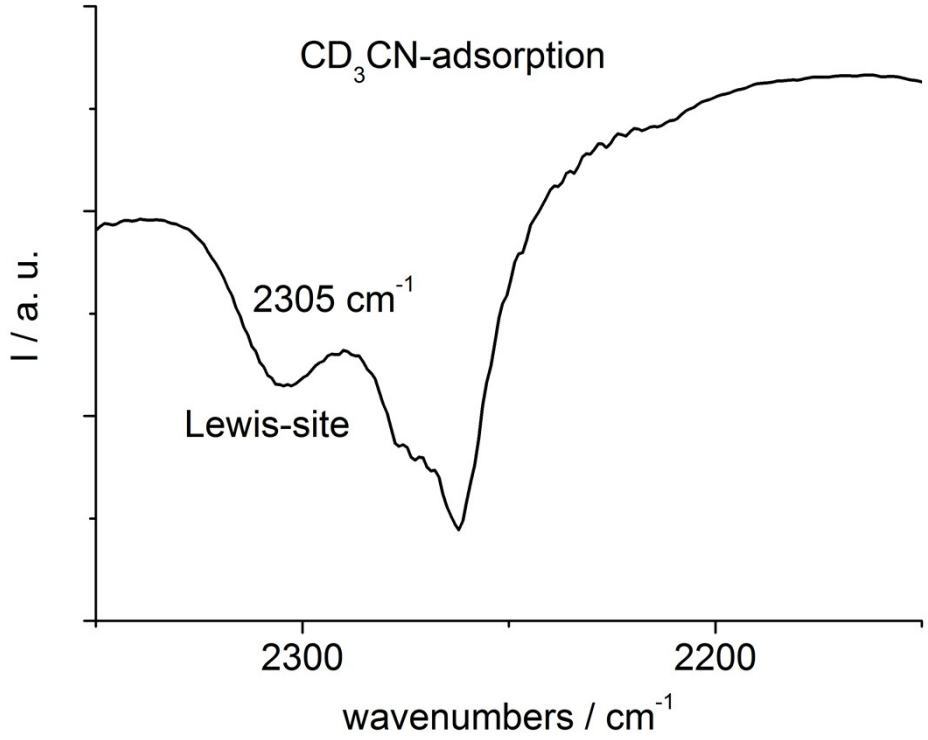

Figure S7: IR spectra for **3** after activation and adsorption of deuterated acetonitrile.

The signal of physisorbed CD_3CN is present at 2260 cm^{-1}. Moreover Brønsted acid sites are observed as indicated by the signal around 2275 cm^{-1}. The Lewis acidic site typical for dehydrated UiO-66-frameworks results in a signal at 2305 cm^{-1}. This indicates a shift by 7 cm^{-1} compared to unfunctionalised UiO-66.[v]

Crystallographic Information.

(1) $[Zr_6(OH)_{10.8}(SO_4)_{3.6}(BDC\text{-}NH_2)_3(H_2O)_{7.4}]\cdot nH_2O$

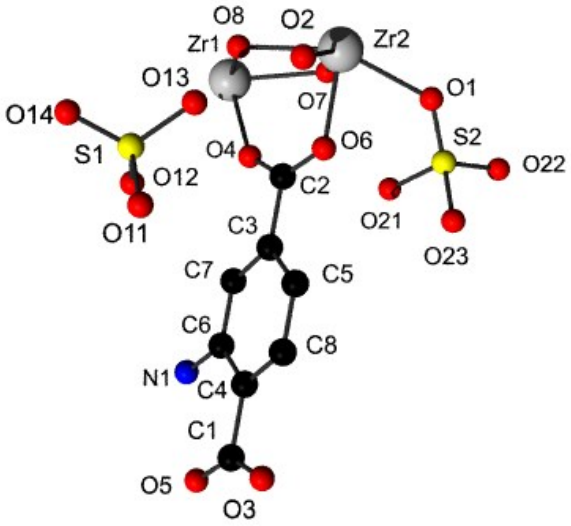

Figure S8: Asymmetric unit of **1** with numbering scheme used in Table S3. Guest molecules are omitted. No standard uncertainties are given for the linker molecules since those were refined as rigid bodies.

Table S3: Some relevant bond distances in the structure of **1**.

Zr1	O8	2.180(20)		O22	1.536(35)
	O3	2.200(14)		O23	1.556(37)
	O4	2.233(11)		O21	1.584(34)
	O7	2.242(20)	C1	O3	1.206(14)
Zr2	O6	2.102(20)		O5	1.232(19)
	O7	2.120(20)		C4	1.539
	O2	2.138(13)	C2	O4	1.252(11)
	O5	2.160(21)		O6	1.254(19)
	O8	2.242(21)		C3	1.5392
	O8	2.259(20)	C3	C5	1.4165
	O7	2.261(17)		C7	1.4279
	O1	2.272(10)	C4	C6	1.4166
S1	O14	1.447(29)		C8	1.4281
	O12	1.502(43)	C5	C8	1.4187
	O13	1.536(37)	C6	C7	1.4187
	O11	1.583(28)		N1	1.4292
S2	O1	1.511(16)			

(**2**) $[Zr_6(OH)_{14}(BDC\text{-}(CO_2H)_2)_4(H_2O)_2(SO_4)]\cdot nH_2O$

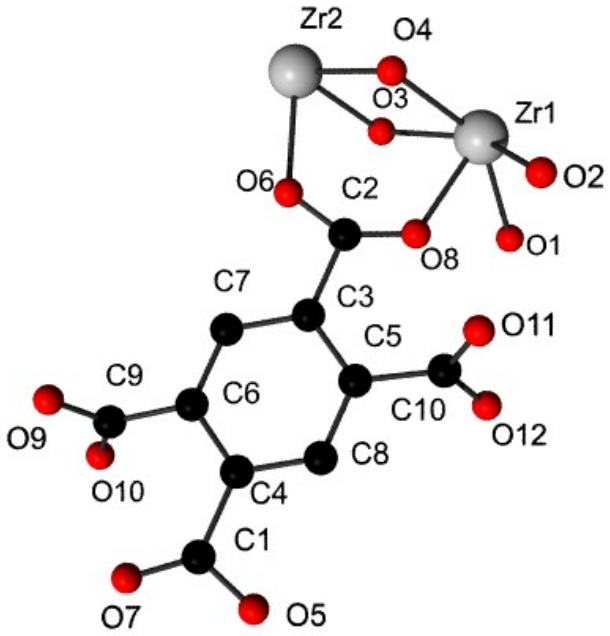

Figure S9: Asymmetric unit of **2** with numbering scheme used in Table S4. Guest molecules are omitted. No standard uncertainties are given for the linker molecules since those were refined as rigid bodies.

Table S4: Some relevant bond distances in the structure of **2**.

Zr1	O7	2.118(8)	C2	O6	1.2198
	O8	2.138(8)		O8	1.2275
	O4	2.165(19)		C3	1.5384
	O3	2.178(21)	C3	C5	1.4085
	O4	2.202(30)		C7	1.4296
	O3	2.204(32)	C4	C6	1.4086
	O1	2.263(16)		C8	1.4298
	O2	2.283(14)	C5	C8	1.4182
Zr2	O4	2.110(17)		C10	1.5005
	O3	2.167(20)	C6	C7	1.4180
	O5	2.222(3)		C9	1.4938
	O6	2.268(3)	C9	O9	1.2648
C1	O7	1.2418		O10	1.2654
	O5	1.2569	C10	O12	1.2632
	C4	1.5382		O11	1.2671

(**3**) $[Zr_6O_2(OH)_6(BDC\text{-}F_4)_6(SO_4)]\cdot n H_2O \cdot 1.2 H_2BDC\text{-}F_4$

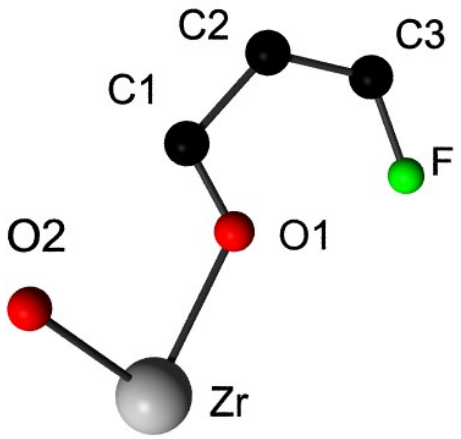

Figure S1: Asymmetric unit of **3** with numbering scheme used in Table S5. Guest molecules are omitted.

Table S5: Some relevant bond distances in the structure of **3**.

Zr	O2	2.208(14)
	O1	2.293(5)
C1	O1	1.252(11)
	C2	1.526(10)
C2	C3	1.439(20)
C3	F	1.393(23)
	C3’	1.416(22)

Crystallographic Information Files.

(1) $[Zr_6(OH)_{10.8}(SO_4)_{3.6}(BDC\text{-}NH_2)_3(H_2O)_{7.4}]\cdot nH_2O$

```
data_
_chemical_name_mineral ZirconiumAminoterephthalateSulfate
_cell_length_a  14.2480(13)
_cell_length_b  14.2480(13)
_cell_length_c  21.3689(25)
_cell_angle_alpha 90
_cell_angle_beta  90
_cell_angle_gamma 90
_cell_volume 4338.00(94)
_symmetry_space_group_name_H-M I-4
loop_
_symmetry_equiv_pos_as_xyz
            '-x, -y, z'
            '-x+1/2, -y+1/2, z+1/2'
            '-y, x, -z'
            '-y+1/2, x+1/2, -z+1/2'
            'y, -x, -z'
            'y+1/2, -x+1/2, -z+1/2'
            'x, y, z'
            'x+1/2, y+1/2, z+1/2'
loop_
_atom_site_label
_atom_site_type_symbol
_atom_site_fract_x
_atom_site_fract_y
_atom_site_fract_z
_atom_site_occupancy
_atom_site_B_iso_or_equiv
Zr1 Zr    0.5 0.5 0.62252(44) 1 0.25(24)
Zr2 Zr    0.62951(35) 0.62819(31) 0.50184(46) 1 0.25(24)
O1 O    0.77918(57) 0.57319(76) 0.5 1 3.17(55)
O2 O    0.6032(14) 0.77587(81) 0.5 1 3.17(55)
O3 O    0.89433(71) 0.90879(83) 0.8335(10) 1 3.17(55)
O4 O    0.60292(73) 0.60942(70) 0.65230(87) 1 3.17(55)
O5 O    0.82207(95) 0.8272(10) 0.91081(90) 1 3.17(55)
O6 O    0.69355(79) 0.68661(94) 0.58141(95) 1 3.17(55)
O7 O    0.6208(12) 0.49168(89) 0.5555(10) 1 3.17(55)
O8 O    0.4994(11) 0.62174(99) 0.5607(12) 1 3.17(55)
C1 C    0.8434173 0.8513637 0.8573124 0.742(19) 2.0(16)
C2 C    0.6653888 0.6657217 0.6352513 0.742(19) 2.0(16)
C3 C    0.7112347 0.7135709 0.6921345 0.742(19) 2.0(16)
C4 C    0.7975712 0.8035131 0.8004393 0.742(19) 2.0(16)
C5 C    0.7733884 0.7905103 0.6854324 0.742(19) 2.0(16)
C6 C    0.7354078 0.7265742 0.8071313 0.742(19) 2.0(16)
C7 C    0.6933102 0.682676 0.7545677 0.742(19) 2.0(16)
C8 C    0.8154958 0.8344094 0.7379962 0.742(19) 2.0(16)
N1 N    0.7134602 0.690987 0.8679285 0.742(19) 2.0(16)
S1 S    0.47708(97) 0.8459(11) 0.65215(61) 0.4777(69) 1.25(97)
O11 O    0.5436(12) 0.9312(19) 0.6690(11) 0.4777(69) 3.17(55)
O12 O    0.4958(12) 0.7756(27) 0.7030(20) 0.4777(69) 3.17(55)
O13 O    0.5146(17) 0.8107(23) 0.5890(17) 0.4777(69) 3.17(55)
O14 O    0.3843(18) 0.8869(17) 0.6493(12) 0.4777(69) 3.17(55)
S2 S    0.8500(12) 0.5521(11) 0.55069(62) 0.4223(69) 1.25(97)
O21 O    0.8066(14) 0.5184(27) 0.6151(15) 0.4223(69) 3.17(55)
O22 O    0.9268(16) 0.4789(27) 0.5379(16) 0.4223(69) 3.17(55)
O23 O    0.9097(22) 0.6341(25) 0.5777(14) 0.4223(69) 3.17(55)
Ow1 O    0.5 0.5 0.986(47) 0.57(65) 3.17(55)
Ow2 O    0.5 0.5 0.941(15) 1.00(63) 3.17(55)
```

(2) $[Zr_6(OH)_{14}(BDC\text{-}(CO_2H)_2)_4(H_2O)_2(SO_4)]\cdot nH_2O$

```
data_
_chemical_name_mineral ZirconiumPyromellitate
_cell_length_a  14.16692(84)
_cell_length_b  14.16692(84)
_cell_length_c  21.4206(15)
_cell_angle_alpha 90
_cell_angle_beta  90
_cell_angle_gamma 90
_cell_volume 4299.15(59)
_symmetry_space_group_name_H-M I-4
loop_
_symmetry_equiv_pos_as_xyz
            '-x, -y, z'
            '-x+1/2, -y+1/2, z+1/2'
            '-y, x, -z'
            '-y+1/2, x+1/2, -z+1/2'
            'y, -x, -z'
            'y+1/2, -x+1/2, -z+1/2'
            'x, y, z'
            'x+1/2, y+1/2, z+1/2'
loop_
_atom_site_label
_atom_site_type_symbol
_atom_site_fract_x
_atom_site_fract_y
_atom_site_fract_z
_atom_site_occupancy
_atom_site_B_iso_or_equiv
Zr1 Zr   0.61979(47) 0.63074(51) 0.50336(36) 1 0.80(16)
Zr2 Zr   0.5 0.5 0.61496(26) 1 0.80(16)
O1 O   0.7794(10) 0.6273(17) 0.5 1 0.80(29)
O2 O   0.5980(13) 0.79032(87) 0.5 1 0.80(29)
O3 O   0.6281(13) 0.5008(24) 0.5597(10) 1 0.80(29)
O4 O   0.4894(23) 0.6222(11) 0.55906(89) 1 0.80(29)
O5 O   0.9021692 0.903834 0.8347605 1 0.80(29)
O6 O   0.591827 0.6052619 0.6666741 1 0.80(29)
O7 O   0.8456837 0.8219044 0.9124056 1 0.80(29)
O8 O   0.6697959 0.6885164 0.5894471 1 0.80(29)
C1 C   0.8497555 0.8396275 0.8556962 1 1.40(79)
C2 C   0.6456136 0.6604207 0.6412437 1 1.40(79)
C3 C   0.6981403 0.706632 0.6961719 1 1.40(79)
C4 C   0.7972302 0.7934257 0.8007781 1 1.40(79)
C5 C   0.7569986 0.7856895 0.6875355 1 1.40(79)
C6 C   0.7383688 0.7143592 0.8093944 1 1.40(79)
C7 C   0.6900813 0.6719899 0.7586299 1 1.40(79)
C8 C   0.8052876 0.8280683 0.7383101 1 1.40(79)
C9 C   0.7389651 0.6732758 0.8736163 1 1.40(79)
O9 O   0.6675366 0.6800828 0.9087479 1 0.80(29)
O10 O   0.8108505 0.6290591 0.8929562 1 0.80(29)
C10 C   0.7708049 0.8244657 0.6229943 1 2
O11 O   0.7045726 0.8687281 0.5960986 1 0.80(29)
O12 O   0.8509669 0.8211209 0.5972629 1 0.80(29)
Ow1 O   0.5454(40) 0.9355(35) 0.7254(25) 1.000(56) 0.80(29)
Ow2 O   0 0.5 0.75 1.00(17) 0.80(29)
Ow3 O   0.4563(38) 0.8699(36) 0.5929(23) 1.000(61) 0.80(29)
Ow4 O   0.5 0.5 0.1960(48) 0.440(45) 0.80(29)
Ow5 O  0 0.4987(59) 0.8243(34) 0.6428(21) 1.000(60) 0.80(29)
```

(3) $[Zr_6O_2(OH)_6(BDC\text{-}F_4)_6(SO_4)]\cdot nH_2O\cdot 1.2H_2BDC\text{-}F_4$

```
data_
_chemical_name_mineral ZirconiumTetrafluoroterephthalate
_cell_length_a  20.82532(44)
_cell_length_b  20.82532(44)
_cell_length_c  20.82532(44)
_cell_angle_alpha 90
_cell_angle_beta  90
_cell_angle_gamma 90
_cell_volume 9031.82(58)
_symmetry_space_group_name_H-M FM-3M
loop_
_symmetry_equiv_pos_as_xyz
            '-x, -y, -z'
            '-x, -y, z'
            '-x, -y+1/2, -z+1/2'
            '-x, -y+1/2, z+1/2'
            '-x, -z, -y'
            '-x, -z, y'
            '-x, -z+1/2, -y+1/2'
            '-x, -z+1/2, y+1/2'
            '-x, z, -y'
            '-x, z, y'
            '-x, z+1/2, -y+1/2'
            '-x, z+1/2, y+1/2'
            '-x, y, -z'
            '-x, y, z'
            '-x, y+1/2, -z+1/2'
            '-x, y+1/2, z+1/2'
            '-x+1/2, -y, -z+1/2'
            '-x+1/2, -y, z+1/2'
            '-x+1/2, -y+1/2, -z'
            '-x+1/2, -y+1/2, z'
            '-x+1/2, -z, -y+1/2'
            '-x+1/2, -z, y+1/2'
            '-x+1/2, -z+1/2, -y'
            '-x+1/2, -z+1/2, y'
            '-x+1/2, z, -y+1/2'
            '-x+1/2, z, y+1/2'
            '-x+1/2, z+1/2, -y'
            '-x+1/2, z+1/2, y'
            '-x+1/2, y, -z+1/2'
            '-x+1/2, y, z+1/2'
            '-x+1/2, y+1/2, -z'
            '-x+1/2, y+1/2, z'
            '-y, -x, -z'
            '-y, -x, z'
            '-y, -x+1/2, -z+1/2'
            '-y, -x+1/2, z+1/2'
            '-y, -z, -x'
            '-y, -z, x'
            '-y, -z+1/2, -x+1/2'
            '-y, -z+1/2, x+1/2'
            '-y, z, -x'
            '-y, z, x'
            '-y, z+1/2, -x+1/2'
            '-y, z+1/2, x+1/2'
            '-y, x, -z'
            '-y, x, z'
            '-y, x+1/2, -z+1/2'
```

'-y, x+1/2, z+1/2'
'-y+1/2, -x, -z+1/2'
'-y+1/2, -x, z+1/2'
'-y+1/2, -x+1/2, -z'
'-y+1/2, -x+1/2, z'
'-y+1/2, -z, -x+1/2'
'-y+1/2, -z, x+1/2'
'-y+1/2, -z+1/2, -x'
'-y+1/2, -z+1/2, x'
'-y+1/2, z, -x+1/2'
'-y+1/2, z, x+1/2'
'-y+1/2, z+1/2, -x'
'-y+1/2, z+1/2, x'
'-y+1/2, x, -z+1/2'
'-y+1/2, x, z+1/2'
'-y+1/2, x+1/2, -z'
'-y+1/2, x+1/2, z'
'-z, -x, -y'
'-z, -x, y'
'-z, -x+1/2, -y+1/2'
'-z, -x+1/2, y+1/2'
'-z, -y, -x'
'-z, -y, x'
'-z, -y+1/2, -x+1/2'
'-z, -y+1/2, x+1/2'
'-z, y, -x'
'-z, y, x'
'-z, y+1/2, -x+1/2'
'-z, y+1/2, x+1/2'
'-z, x, -y'
'-z, x, y'
'-z, x+1/2, -y+1/2'
'-z, x+1/2, y+1/2'
'-z+1/2, -x, -y+1/2'
'-z+1/2, -x, y+1/2'
'-z+1/2, -x+1/2, -y'
'-z+1/2, -x+1/2, y'
'-z+1/2, -y, -x+1/2'
'-z+1/2, -y, x+1/2'
'-z+1/2, -y+1/2, -x'
'-z+1/2, -y+1/2, x'
'-z+1/2, y, -x+1/2'
'-z+1/2, y, x+1/2'
'-z+1/2, y+1/2, -x'
'-z+1/2, y+1/2, x'
'-z+1/2, x, -y+1/2'
'-z+1/2, x, y+1/2'
'-z+1/2, x+1/2, -y'
'-z+1/2, x+1/2, y'
'z, -x, -y'
'z, -x, y'
'z, -x+1/2, -y+1/2'
'z, -x+1/2, y+1/2'
'z, -y, -x'
'z, -y, x'
'z, -y+1/2, -x+1/2'
'z, -y+1/2, x+1/2'
'z, y, -x'
'z, y, x'
'z, y+1/2, -x+1/2'
'z, y+1/2, x+1/2'
'z, x, -y'

'z, x, y'
'z, x+1/2, -y+1/2'
'z, x+1/2, y+1/2'
'z+1/2, -x, -y+1/2'
'z+1/2, -x, y+1/2'
'z+1/2, -x+1/2, -y'
'z+1/2, -x+1/2, y'
'z+1/2, -y, -x+1/2'
'z+1/2, -y, x+1/2'
'z+1/2, -y+1/2, -x'
'z+1/2, -y+1/2, x'
'z+1/2, y, -x+1/2'
'z+1/2, y, x+1/2'
'z+1/2, y+1/2, -x'
'z+1/2, y+1/2, x'
'z+1/2, x, -y+1/2'
'z+1/2, x, y+1/2'
'z+1/2, x+1/2, -y'
'z+1/2, x+1/2, y'
'y, -x, -z'
'y, -x, z'
'y, -x+1/2, -z+1/2'
'y, -x+1/2, z+1/2'
'y, -z, -x'
'y, -z, x'
'y, -z+1/2, -x+1/2'
'y, -z+1/2, x+1/2'
'y, z, -x'
'y, z, x'
'y, z+1/2, -x+1/2'
'y, z+1/2, x+1/2'
'y, x, -z'
'y, x, z'
'y, x+1/2, -z+1/2'
'y, x+1/2, z+1/2'
'y+1/2, -x, -z+1/2'
'y+1/2, -x, z+1/2'
'y+1/2, -x+1/2, -z'
'y+1/2, -x+1/2, z'
'y+1/2, -z, -x+1/2'
'y+1/2, -z, x+1/2'
'y+1/2, -z+1/2, -x'
'y+1/2, -z+1/2, x'
'y+1/2, z, -x+1/2'
'y+1/2, z, x+1/2'
'y+1/2, z+1/2, -x'
'y+1/2, z+1/2, x'
'y+1/2, x, -z+1/2'
'y+1/2, x, z+1/2'
'y+1/2, x+1/2, -z'
'y+1/2, x+1/2, z'
'x, -y, -z'
'x, -y, z'
'x, -y+1/2, -z+1/2'
'x, -y+1/2, z+1/2'
'x, -z, -y'
'x, -z, y'
'x, -z+1/2, -y+1/2'
'x, -z+1/2, y+1/2'
'x, z, -y'
'x, z, y'
'x, z+1/2, -y+1/2'

```
            'x, z+1/2, y+1/2'
            'x, y, -z'
            'x, y, z'
            'x, y+1/2, -z+1/2'
            'x, y+1/2, z+1/2'
            'x+1/2, -y, -z+1/2'
            'x+1/2, -y, z+1/2'
            'x+1/2, -y+1/2, -z'
            'x+1/2, -y+1/2, z'
            'x+1/2, -z, -y+1/2'
            'x+1/2, -z, y+1/2'
            'x+1/2, -z+1/2, -y'
            'x+1/2, -z+1/2, y'
            'x+1/2, z, -y+1/2'
            'x+1/2, z, y+1/2'
            'x+1/2, z+1/2, -y'
            'x+1/2, z+1/2, y'
            'x+1/2, y, -z+1/2'
            'x+1/2, y, z+1/2'
            'x+1/2, y+1/2, -z'
            'x+1/2, y+1/2, z'
loop_
_atom_site_label
_atom_site_type_symbol
_atom_site_fract_x
_atom_site_fract_y
_atom_site_fract_z
_atom_site_occupancy
_atom_site_B_iso_or_equiv
Zr Zr    0.12214(19) 0 0 1 0.20(11)
O1 O    0.17603(43) 0 0.09600(25) 1 4.44(33)
O2 O    0.06152(64) -0.06152(64) -0.06152(64) 1 4.44(33)
C3 C    0.26583(29) 0.0215(10) 0.18611(30) 0.5 0.40(52)
C1 C    0.15037(32) 0 -0.15037(32) 1 0.40(52)
C2 C    0.20217(33) 0 0.20217(33) 1 0.40(52)
F F    0.37597(50) 0.71382(57) 0.46400(65) 0.5 8.00(72)
Ow1 O    0.2624(14) 0.5 0.5 0.845(25) 4.44(33)
Ow2 O    0.36321(71) 0.63679(71) 0.78702(95) 0.463(11) 4.44(33)
```

References

[i] Materials Studio Version 5.0, Accelrys Inc., San Diego, CA, 2009.

[ii] Topas Academics 4.2, Coelho Software, 2007.

[iii] W. Kraus, G. Nolze, PowderCell 2.4, 2000.

[iv] N. Reimer, B. Gil, B. Marszalek, N. Stock, *CrystEngComm*, 2012, **14**, 4119.

[v] F. Vermoortele, B. Bueken, G. Le Bars, B. Van de Voorde, M. Vandichel, K. Houthoofd, A. Vimont, M. Daturi, M. Waroquier, V. Van Speybroeck, C. Kirschhock, D. De Vos, *J. Am. Chem. Soc.*, 2013, **135**, 11465